Supporting Information

for

Antibonding Cu (*d*)-Te (*p*) states and bonding inhomogeneity in inducing low lattice thermal conductivity and extraordinary thermoelectric properties of layered heteroanionic NdCuOTe material: A first-principles study

Shuwei Tang,*[a,b] Wanrong Guo,[a] Da Wan,[a] Xiaodong Li,[a] Tuo Zheng,[a] Hao Wang,[a] Qingshun Li,[a] Xiuling Qi,[a] and Shulin Bai*[a]

[a]College of Materials Science and Engineering, Liaoning Technical University, Fuxin, Liaoning 123000, China.
[b]Faculty of Chemistry, Northeast Normal University, Changchun, Jilin 130024, China.

Corresponding author:

Shuwei Tang
E-mail: tangsw911@nenu.edu.cn

Shulin Bai
E-mail: baishulin@buaa.edu.cn

College of Materials Science and Engineering
Liaoning Technical University
Zhonghua Road. #47
Fuxin, Liaoning
123000, China
Tel/Fax: +86-418-5110098

Contents

Section 1. Computational parameters for carrier transport property

1. Scattering mechanism calculational details

In order to accurately describe the electronic transport properties, different scattering mechanisms, including the acoustic deformation potential (ADP), ionized impurity (IMP) and polar optical (POP) scattering were considered into the calculation of electronic transport parameters. The differential scattering rate from state $|n\mathbf{k}\rangle$ to state $|m\mathbf{k}+\mathbf{q}\rangle$ was calculated by the AMSET code[1] within the Born approximation using Fermi's golden rule:

$$W_{n\mathbf{k}\to m\mathbf{k}+\mathbf{q}} = \frac{2\pi}{\hbar}\left|g_{nm}(\mathbf{k},\mathbf{q})\right|^2 \delta(\varepsilon_{n\mathbf{k}} - \varepsilon_{m\mathbf{k}+\mathbf{q}}) \quad (1)$$

where the symbols denote the band index (n and m), wave vector (**k**, **k** + **q**), reduced Planck's constant ($\hbar$), electron energy (ε), Dirac delta function (δ), coupling matrix element (g), respectively. The $\varepsilon_{n\mathbf{k}}$ and g_{nm} (**k**, **q**) represent the energy of state $|n\mathbf{k}\rangle$ and the matrix element for scattering from state $|n\mathbf{k}\rangle$ into state $|m\mathbf{k}+\mathbf{q}\rangle$, respectively. The total mode-dependent scattering rate is obtained by integrating the scattering rate over the entire Brillouin zone. The differential scattering rate for inelastic processes was calculated as follows:

$$W_{n\mathbf{k}\to m\mathbf{k}+\mathbf{q}} = \frac{2\pi}{\hbar}\left|g_{nm}(\mathbf{k},\mathbf{q})\right|^2 \times \left[(n_{\mathrm{po}}+1-f_{m\mathbf{k}+\mathbf{q}})\delta(\varepsilon_{n\mathbf{k}} - \varepsilon_{m\mathbf{k}+\mathbf{q}} - \hbar\omega_{\mathrm{po}}) \right. \quad (2)$$
$$\left. (n_{\mathrm{po}}+f_{m\mathbf{k}+\mathbf{q}})\delta(\varepsilon_{n\mathbf{k}} - \varepsilon_{m\mathbf{k}+\mathbf{q}} - \hbar\omega_{\mathrm{po}})\right]$$

where ω_{po} is an effective phonon frequency, n_{po} is the Bose-Einstein distribution of the phonons, $-\hbar\omega_{\mathrm{po}}$ and $+\hbar\omega_{\mathrm{po}}$ terms correspond to scattering by phonon absorption and emission, respectively. The ADP scattering describes the interaction between phonons and electrons, which was calculated using the *n*-type and *p*-type deformation potentials as well as the elastic constants:[2,3]

$$g_{nm}^{\mathrm{ad}}(\mathbf{k},\mathbf{q}) = \sqrt{k_{\mathrm{B}}T}\sum_{\mathbf{G}\neq-\mathbf{q}}\left[\frac{\mathbf{D}_{n\mathbf{k}}:\hat{\mathbf{S}}_{l}}{c_{l}\sqrt{\rho}} + \frac{\mathbf{D}_{n\mathbf{k}}:\hat{\mathbf{S}}_{t_1}}{c_{t_1}\sqrt{\rho}} + \frac{\mathbf{D}_{n\mathbf{k}}:\hat{\mathbf{S}}_{t_2}}{c_{t_2}\sqrt{\rho}}\right]\left\langle m\mathbf{k}+\mathbf{q}\left|e^{i(\mathbf{q}+\mathbf{G})\cdot\mathbf{r}}\right|n\mathbf{k}\right\rangle \backslash^{*}$$

MERGEFORMAT (3)

where $\mathbf{D}_{n\mathbf{k}}$ represents the rank 2 deformation potential tensor, **S** symbolizes the unit strain associated with an acoustic mode, and the subscripts (l, t_1, t_2) imply properties belonging to the longitudinal and transverse modes. The POP scattering involves the interaction between polar optical phonons and electrons. Based on the polar optical phonon frequency, static and high-frequency dielectric constants, the differential scattering rate of polar optical phonons was given by the following equation:[2,4,5]

$$g_{nm}^{\mathrm{po}}(\mathbf{k},\mathbf{q}) = \left[\frac{\hbar\omega_{\mathrm{po}}}{2}\right]^{1/2}\sum_{\mathbf{G}\neq-\mathbf{q}}\left(\frac{1}{\hat{\mathbf{n}}\cdot\varepsilon_{\infty}\cdot\hat{\mathbf{n}}} - \frac{1}{\hat{\mathbf{n}}\cdot\varepsilon_{\mathrm{S}}\cdot\hat{\mathbf{n}}}\right)^{\frac{1}{2}}\frac{\left\langle m\mathbf{k}+\mathbf{q}\left|e^{i(\mathbf{q}+\mathbf{G})\cdot\mathbf{r}}\right|n\mathbf{k}\right\rangle}{\left|\mathbf{q}+\mathbf{G}\right|}\backslash^{*}$$

MERGEFORMAT (4)

where $\boldsymbol{\varepsilon}_{\mathrm{S}}$ and $\boldsymbol{\varepsilon}_{\infty}$ represent the static and high-frequency dielectric tensors, and the ω_{po} denotes the polar optical phonon frequency. In order to capture the full scattering profile of the phonon dispersion, it is necessary to weight each phonon mode according to the dipole moment. The IMP scattering considers the scattering of ionized charge carriers and the matrix element that was defined based on the static dielectric constant:[2,6]

$$g_{nm}^{\mathrm{ii}}(\mathbf{k},\mathbf{q}) = \sum_{\mathbf{G}\neq-\mathbf{q}}\frac{n_{\mathrm{ii}}^{1/2}Ze}{\hat{\mathbf{n}}\cdot\varepsilon_{\mathrm{S}}\cdot\hat{\mathbf{n}}}\frac{\left\langle m\mathbf{k}+\mathbf{q}\left|e^{i(\mathbf{q}+\mathbf{G})\cdot\mathbf{r}}\right|n\mathbf{k}\right\rangle}{\left|\mathbf{q}+\mathbf{G}\right|^{2}+\beta^{2}}\backslash^{*}$$

MERGEFORMAT (5)

where Z represents the charge state at the centre of the impurity, n_{ii} denotes the concentration of the ionized impurity, and β stands for the inverse shielding length. Based on the elastic constants, deformation potentials tensor, dielectric constants, piezoelectric constants, polar-phonon frequency, and the wave function coefficients obtained from the electronic band structure in **Table S1** of **Supporting Information**, the carrier relaxation time was computed by the AMSET software.

2. Electronic transport calculation details

Table S1. The parameters for the electronic transport calculation within AMSET code.

AMSET parameters			
Deformation potential tensor (Valence band maximum)	$\begin{bmatrix} 1.34 & 1.87 & 1.86 \\ 1.87 & 0.02 & 1.86 \\ 1.86 & 1.86 & 1.75 \end{bmatrix}$	Deformation potential tensor (Conduction band minimum)	$\begin{bmatrix} 2.32 & 2.74 & 5.09 \\ 2.74 & 1.08 & 2.73 \\ 5.09 & 2.73 & 0.85 \end{bmatrix}$
High-frequency dielectric constant tensor (ε_0)	$\begin{bmatrix} 9.47 & 0 & 0 \\ 0 & 9.47 & 0 \\ 0 & 0 & 8.01 \end{bmatrix}$	Static dielectric constant tensor (ε_0)	$\begin{bmatrix} 18.76 & 0 & 0 \\ 0 & 18.76 & 0 \\ 0 & 0 & 17.94 \end{bmatrix}$
Elastic constant tensor (GPa)	$\begin{bmatrix} 157.2 & 52.9 & 55.4 & 0 & 0 & 0 \\ 52.9 & 157.2 & 55.4 & 0 & 0 & 0 \\ 55.4 & 55.4 & 91.5 & 0 & 0 & 0 \\ 0 & 0 & 0 & 9.0 & 0 & 0 \\ 0 & 0 & 0 & 0 & 9.0 & 0 \\ 0 & 0 & 0 & 0 & 0 & 38.9 \end{bmatrix}$		
Polar optical phonon frequency (THz)	0.47		
Piezoelectric constant (C/m^2)	$\begin{bmatrix} 0 & 0 & 0 & 0 & 0 & 0 \\ 0 & 0 & 0 & 0 & 0 & 0 \\ 0 & 0 & 0 & 0 & 0 & 0 \end{bmatrix}$		

Section 2. Ab initio molecular dynamics (AIMD) simulations

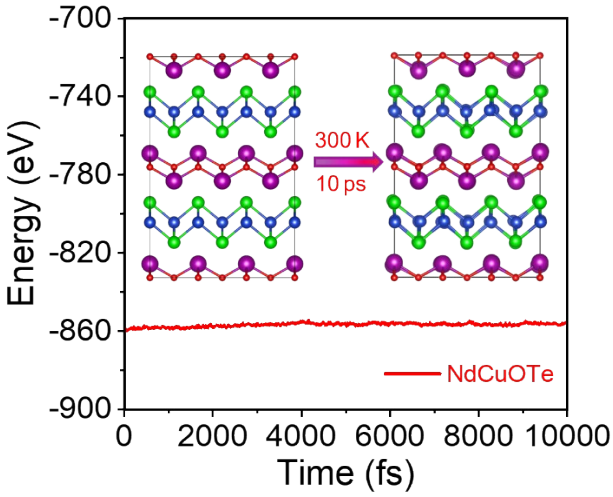

Figure S1. The snapshots of the ab initio molecular dynamics (AIMD) simulations of the NdCuOTe material at 300 K.

Section 3. Electronic band structures calculations

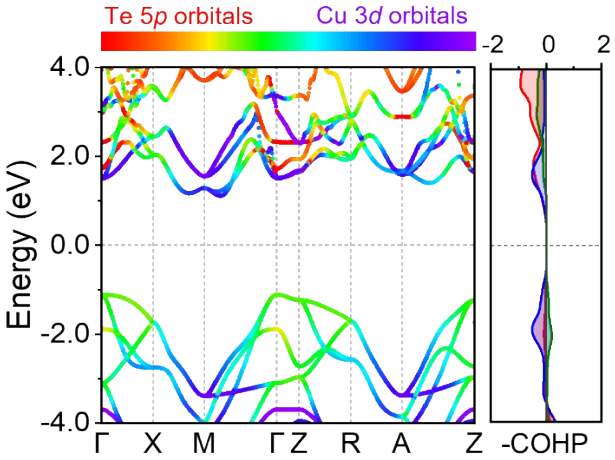

Figure S2. The orbital-projected band structures and -COHP of the NdCuOTe material.

Section 4. Calculation parameters for mechanical properties

Based on the elastic constant in **Table S2**, the bulk modulus (B) and shear modulus (G) of NdCuOTe are computed using the Voigt (V), Reuss (R), and Voigt-Reuss-Hill methods, as outlined in **Table S3**:[7-9]

$$B_V = \frac{1}{9}\left[2\left(C_{11}+C_{12}\right)+C_{33}+4C_{13}\right] \quad \text{* MERGEFORMAT (6)}$$

$$G_V = \frac{1}{30}\left(M+3C_{11}-3C_{12}+12C_{44}+6C_{66}\right) \quad \text{* MERGEFORMAT (7)}$$

$$B_R = \frac{C^2}{M} \quad \text{* MERGEFORMAT (8)}$$

$$G_R = 15\left(\frac{18B_V}{C^2}+\frac{6}{C_{11}-C_{12}}+\frac{6}{C_{44}}+\frac{3}{C_{66}}\right)^{-1} \quad \text{* MERGEFORMAT (9)}$$

$$M = C_{11}+C_{12}+2C_{33}-4C_{13} \quad \text{* MERGEFORMAT (10)}$$

$$C^2 = \left(C_{11}+C_{12}\right)C_{33}-2C_{13}^2 \quad \text{* MERGEFORMAT (11)}$$

$$B_H = \frac{B_V+B_R}{2} \quad \text{* MERGEFORMAT (12)}$$

$$G_H = \frac{G_V+G_R}{2} \quad \text{* MERGEFORMAT (13)}$$

According to Hill approach,[9] the B value measures the resistance to deformation under external compression. Notably, the NdCuOTe material has a commendable B value, showcasing the capability of maintaining volume and shape against compression. The NdCuOTe (B_H=78.9 GPa) material demonstrates a larger B_H value in comparison with YZnAsO (74.0 GPa) material,[10] showing a relatively low compressibility. Meanwhile, compared with LaOCuSe (G_H=37.1 GPa) and BiOCuSe (G_H=34.7 GPa) materials,[11] NdCuOTe material exhibits a relatively smaller G_H of 22.0 GPa, which suggests a weaker stiffness and covalent bonding character. More importantly, the B_H value for NdCuOTe material is considerably larger than the G_H, indicating a high resistance to deformation. The Cauchy pressure (C_{12} - C_{44}) and Pugh's ratio (B/G) for NdCuOTe material is 43.9 GPa and 3.59, respectively, showcasing a ductile feature.[12]

Subsequently, the Young's modulus (E) and Poisson's ratio (ν) are assessed, as presented in **Table S4**:[13]

$$E = \frac{9BG}{3B+G} \qquad \text{* MERGEFORMAT (14)}$$

$$\nu = \frac{3B-2G}{6B+2G} \qquad \text{* MERGEFORMAT (15)}$$

The E of NdCuOTe material under the H approximation is 60.3 GPa, suggesting the inherent rigidity and enhanced resistance to deformation. The Poisson's ratio is 0.37, suggesting the ductile characteristics of NdCuOTe material, consistent with the analysis of Cauchy pressure and Pugh's ratio. The anisotropy in compressibility and shear for NdCuOTe material is evaluated based on the differences in crystal structure arrangement along the in-plane and out-of-plane directions, using the equations proposed by Chung and Buessem:[14]

$$A_C = \frac{B_V - B_R}{B_V + B_R} \qquad \text{* MERGEFORMAT (16)}$$

$$A_S = \frac{G_V - G_R}{G_V + G_R} \qquad \text{* MERGEFORMAT (17)}$$

The A_C and A_S for NdCuOTe material are 3.3% and 25.3%, respectively, which are comparable to the counterparts in BiOCuSe (2.6% and 2.4%) material,[5] demonstrating the pronounced elastic anisotropy, particularly in terms of shear resistance properties. **Figure S3** presents the three-dimensional surface (3D space) and a projected 2D surface (in-plane) for NdCuOTe material, where the B, E and G along different directions are delineated by the following equations:[15,16]

$$\frac{1}{B} = (S_{11}+S_{12}+S_{13})(l_1^2+l_2^2) - (2S_{13}+S_{33})l_3^2 \text{* MERGEFORMAT (18)}$$

$$\frac{1}{E} = S_{11}(l_1^4+l_2^4) + (2S_{13}+S_{44})(l_1^2l_3^2+l_2^2l_3^2) + S_{33}l_3^4 + (2S_{12}+S_{66})l_1^2l_2^2 \text{* MERGEFORMAT (19)}$$

$$\frac{1}{G} = S_{44} + \left[(S_{11}-S_{12}) - \frac{S_{44}}{2}\right](1-l_3^2) + 2(S_{11}+S_{33}-2S_{13}-S_{44})l_3^2(1-l_3^2) \text{* MERGEFORMAT (20)}$$

In these equations, the flexibility matrix S_{ij} is defined as the inverse matrix of the stiffness matrix C_{ij}, l_1, l_2 and l_3 denote the cosines along the *a*-, *b*- and *c*-axis directions, respectively. Notably, the NdCuOTe material exhibits a more pronounced anisotropy along the in-plane and out-of-plane directions. The maximum and minimum for *B* are 120.9 GPa along the in-plane direction and 43.9 GPa along the out-of-plane direction, respectively, which results in an anisotropy ratio of 2.75 for NdCuOTe material. Meanwhile, the corresponding *G* values are 52.0 and 9.0 GPa, respectively, yielding an anisotropy ratio of 5.79. Similar situation is also observed for Young's moduli of NdCuOTe material, which are 120.1 and 31.0 GPa, respectively, associating with an anisotropy ratio of 3.88. Overall, the heightened mechanical anisotropy along the in-plane and out-of-plane directions of the NdCuOTe material is beneficial for generating high anharmonic dispersion of phonons.

Table S2. Elastic constant (C_{ij}, GPa) and compliance constant (S_{ij}, GPa^{-1}) in NdCuOTe material.

System	C_{11}	C_{12}	C_{13}	C_{33}	C_{44}	C_{66}	S_{11}	S_{12}	S_{13}	S_{33}	S_{44}	S_{66}
NdCuOTe	157.2	52.9	55.4	91.5	9.0	38.9	0.0083	-0.0013	-0.0042	0.016	0.11	0.026

Table S3. Bulk modulus (B_T, GPa) and Shear modulus (G_T, GPa) for the NdCuOTe, where *T* are *V*, *R*, and *H* for the Voigt, Reuss, and Voigt-Reuss-Hill approaches, respectively.

System	B_V	B_R	B_H	G_V	G_R	G_H	B_V/G_V	B_R/G_R	B_H/G_H
NdCuOTe	81.5	76.3	78.9	27.5	38.9	16.4	2.96	4.65	4.81

Table S4. Elastic constant (C_{ij}, GPa) and compliance constant (S_{ij}, GPa^{-1}) in NdCuOTe material. Young's modulus (E_T, GPa) and Poisson ratio (v_T) for the NdCuOTe, where *T* are *V*, *R*, and *H* for the Voigt, Reuss, and Voigt-Reuss-Hill approaches, respectively.

System	E_V	E_R	E_H	v_V	v_R	v_H
NdCuOTe	74.2	45.9	60.3	0.35	0.40	0.37

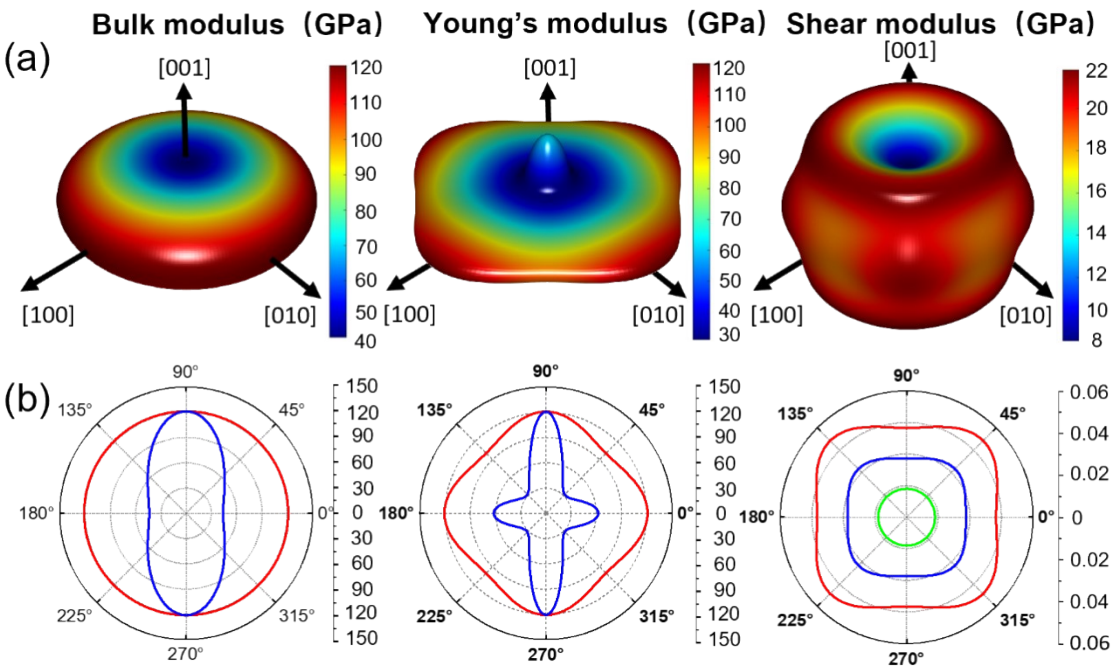

Figure S3. (a)Anisotropic mechanical properties (bulk modulus, Young's modulus, and shear modulus) of the NdCuOTe material in the 3D spatial phase. (b) The mechanical properties (bulk modulus, Young's modulus, and shear modulus) projected onto in-plane direction.

References

1 A. M. Ganose, J. Park, A. Faghaninia, R. Woods-Robinson, K. A. Persson and A. Jain, *Nat. Commun.*, 2021, **12**, 2222.

2 D. L. Rode, in *Semiconductors and Semimetals*, ed. R. K. Willardson and A. C. Beer, Elsevier, 1975, vol. 10, pp. 1-89.

3 J. Bardeen and W. Shockley, *Phys. Rev.*, 1950, **80**, 72-80.

4 H. Fröhlich, *Adv. Phys.*, 1954, **3**, 325-361.

5 E. M. Conwell, *Solid State Pbysics*, 1967.

6 R. B. Dingle, *Lond. Edinb. Dubl. Phil. Mag*, 1955, **46**, 831-840.

7 W. Voigt, in *Lehrbuch der Kristallphysik* (*mit Ausschluß der Kristalloptik*), ed. W. Voigt, Springer, Wiesbaden, 1966.

8 A. Reuss, *Zamm-z Angew Math Me*, 1929, **9**, 49-58.

9 R. Hill, *Proc. Phys. Soc., Sect. A*, 1952, **65**, 349.

10 S. Sau, S. S. Sahoo, A. R. Natarajan and V. Kanchana, *Physica B*, 2023, **657**, 414811.

11 S. K. Saha and G. Dutta, *Phys. Rev. B*, 2016, **94**, 125209.

12 S. F. Pugh, *Lond. Edinb. Dubl. Phil. Mag.*, 1954, **45**, 823-843.

13 M. Shafiullah, S. U. Haq, R. Muhammad, M. Faizan, A. Laref, W. Derafa, A. Sohail, A. Khesro and A. Samad, *Phys. Scr.*, 2023, **98**, 065922.

14 D. H. Chung and W. R. Buessem, *J. Appl. Phys.*, 1967, **38**, 2010-2012.

15 D. Heciri, H. Belkhir, R. Belghit, B. Bouhafs, R. Khenata, R. Ahmed, A. Bouhemadou, T. Ouahrani, X. Wang and S. B. Omran, *Mater. Chem. Phys.*, 2019, **221**, 125-137.

16 X. Liu and J. Fu, *Optik*, 2020, **206**, 164342.